34th Annual International Conference of the IEEE EMBS
San Diego, California USA, 28 August - 1 September, 2012

Quantitative Volumetric Breast Imaging with 3D Inverse Scatter Computed Tomography*

Michael André, James Wiskin, David Borup, Steven Johnson, Haydee Ojeda-Fournier and Linda Olson

Abstract— **A method was developed to map tissue properties of the entire breast including sound speed and attenuation using fully 3D nonlinear inverse-scattering tomography. Clinical measurements suggest that in breast tissue benign and cancerous lesions may be identified in part by these inherent acoustic parameters. Sound speed accuracy and linearity are very high over a wide range (1325-1700 m/sec) with ~1.5 mm resolution at 2 MHz in transmission mode. Attenuation tomograms provide image contrast over a wide range (0-4 dB/cm/MHz) and assist classification of masses. High resolution 0.6 mm volumetric reflection tomograms are acquired with bandwidth 2-8 MHz, are refraction-corrected with the transmission tissue data and are precisely registered in 3D with the transmission volumes. USCT promises an automated whole-breast scan providing a global view of the entire breast in 3D, facilitating comparison to prior exams in a reproducible geometry. Scanner design, automated operation and results of our trial with over 125 subjects with confirmed breast masses will be presented with detailed comparison to conventional sonography and MRI.**

I. Introduction

Conventional breast sonography is the principal adjunctive imaging modality to mammography, both for secondary screening and for diagnostic workup of suspected findings. However, it is a difficult exam to perform and the quality is dependent on the skill of the operator as well as technical features of the scanner. Conventional sonography devices produce images of reflected and backscattered ultrasound energy, or relative "echogenicity." The major strength of breast ultrasound and its most common use is differentiation of cystic and solid lesions with nearly 100% accuracy [1-3]. Nonetheless, numerous studies of conventional breast ultrasound show substantial variance in diagnostic accuracy due to variability in radiologists' skill levels [4] and technical features of the scanner [5]. Even with the best imaging methods available today, up to 80% of breast biopsies performed turn out to be benign [6]. Combined mammography and targeted breast ultrasound is still the most effective approach for breast cancer screening in women at normal risk [7,8]. Adding a single screening ultrasound to mammography yields an additional 1.1 to 7.2 detected cancers per 1000 high risk women, but at a substantial increase in false positives [9,10]. Sonography is not usually employed for screening due to procedural complexity, additional skill required and cost. In order to obtain the needed high resolution, the field of view in sonography is very small, which greatly complicates interpretation, localization of masses and comparison to prior exams. These same drawbacks may limit shear wave speed methods in elastography.

*Research supported by DHHS NIH/NCI 1 R44 CA 110203-01A2.

M. A., H. O., L. O. Authors are with the Departments of Radiology, University of California and Veterans Affairs Medical Center, San Diego, CA 92093 USA (858-552-8585; e-mail: mandre@ucsd.edu).

J. W., D. B., S. J. Authors, are with Techniscan Medical Systems, Inc., and J.W. also with the Department of Bioengineering, University of Utah, Salt Lake City, UT 84106 USA (e-mail: j.w.wiskin@gmail.com).

II. Ultrasound Computed Tomography

Whole breast ultrasound computed tomography (USCT) using transmission or reflection techniques has been proposed for many years as a means to address these shortcomings. Research has shown great potential for accurate spatial registration, high spatial and contrast resolution, minimal artifacts and quantitative tissue measurements, particularly sound speed, attenuation and morphometry. The research has also illustrated it is a difficult, inherently non-linear and three-dimensional (3D) problem. The historical approaches to USCT can be grouped in three categories.

A. Ray-Based Backprojection

Early attempts to use time of flight (TOF) measurements along rays combined with computed tomography reconstruction were analogous to x-ray CT [11-15]. In this case, back-projection of the integrated TOF and attenuation data along straight, or in some cases curved rays, allowed more accurate, quantitative tissue imaging. The method has low spatial resolution due to lack of compensation for diffraction. A further flaw is that true image inversion is a nonlinear process, not easily amenable to linear approximations.

B. Diffraction Tomography

In general, due to limitations of instrumentation and algorithms, the second stage in development of ultrasound transmission imaging was to use two-dimensional linearization techniques to solve wave equations, rather than geometrical ray models. This approach usually fails for breasts because it is based on first-order perturbation (Born or Rytov) approximations [16-18] that are valid only for small variations in sound speed and attenuation.

C. Inverse Scatter Tomography (IST)

The third stage of development is the introduction of true wave equation based methods (not linear perturbation approximations) as models of ultrasound wave propagation

[19,20]. The wave equation approach provides a non-linear model of considerable accuracy, compensates for multiple scattering and provides constant resolution throughout the image volume. This model is inverted by an iterative simultaneous determination of the breast tissue parameters and internal total fields (Fig. 1). Until recently, the mathematical and technical challenges for full-wave 3D IST were so complex that practical results in humans were not realized.

Figure 1. General inverse scatter algorithm

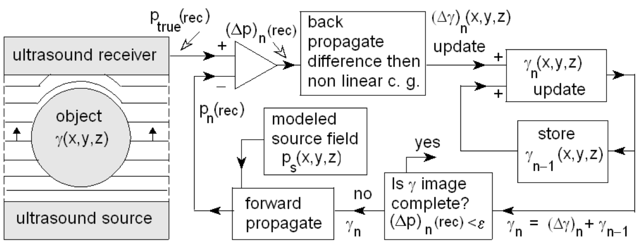

A practical scanner employing IST imaging was developed by Techniscan Medical Systems (TMS, Salt Lake City, UT) [21-24]. To achieve a solution of the inverse scattering problem the algorithm implements a fast forward solver and concomitant methods for large scale minimization (~20 million unknowns), which is based on the Ribiere-Polak version of nonlinear conjugate gradients. To solve the numerically ill-conditioned problem of full-wave inversion, increasing discrete frequency data are used and the number of iterations can be reduced by preconditioning to a practical level of 5-8 to achieve a 5% residual. The method does not account for density variations but for scatter in the forward direction this approximation has proven reasonable. Detailed description of the IST algorithm is published elsewhere [20,24,25].

D. *Reflection Tomography (RT)*

The scanner includes a set of three transceiver arrays that are coincident with the transmission arrays to simultaneously acquire conventional B-scan data. The arrays have a bandwidth of ~2-8 MHz and are focused at different depths to provide complete coverage of the breast. A high-resolution RT algorithm was developed that utilizes the sound speed image to correct for refraction and attenuation images to adjust amplitude along the ray. The resulting backprojected RT image is a 360° compound B-scan.

III. Materials and Methods

A. *Data Acquisition*

The current TMS scanner that is the subject of this paper is being examined at University of California, San Diego (UCSD), Mayo Clinic, Rochester, MN, and University of Freiburg, Germany to evaluate clinical feasibility of using IST and RT to analyze and detect breast masses as well as monitor changes due to therapies. All of the data presented here is from UCSD.

The TMS scanner (Fig. 2) provides an automated, standardized scan of the whole breast nearly independent of operator expertise. The patient lies prone with her breast pendant but docked to a retention rod in a controlled 31°C water bath within the field of view of several transducer arrays. The IST transmitter and receiver array rotate around 360° to collect 180 tomographic views of ultrasound wave data (Fig. 3). The transmitter emits broad-band plane pulses (0.3-2 MHz) while the receiver array, comprised of 1536 elements in 8 vertical rows, digitizes the time signal. Three coincident RT arrays (5MHz center, 80% bandwidth) spaced at 48° are angled upward at 12° to access the chest wall. Scan time is ~10-20 sec per level, ~8 min for the average breast. 3D transmission and aberration-corrected RT reconstructions are accomplished in ~40 minutes employing 2 GPUs for a portion of the process.

Figure 2. IST scanner with transducer arrays in water tank

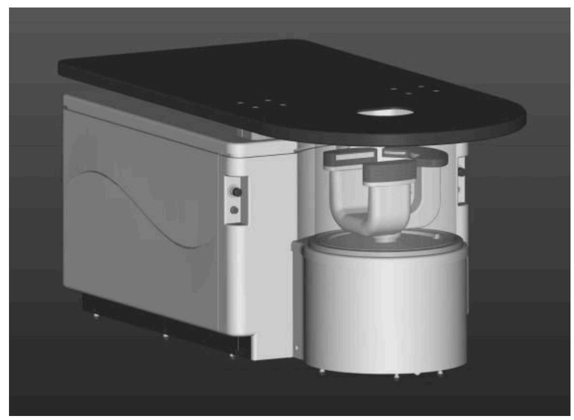

Figure 3. Transducer arrangement

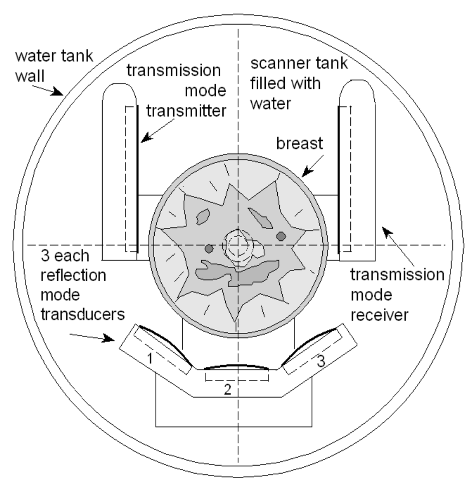

B. *Patient Study Population*

Female patients recruited to the IRB-approved protocol were referred for a diagnostic breast sonogram as the result of prior findings on mammography, physical exam or previous known conditions. The purpose of the study was to measure a range of tissue properties in women with widely varying breast sizes and mammographic densities, to assess reproducibility of findings and to examine depiction and quantitative properties of masses confirmed by biopsy or long-term benign follow-up. The statistical design was to assess equivalence to sonography (93% power).

IV. RESULTS

A. *Scanner Performance*

All reported results are from the TMS scanner at UCSD. 2D reconstruction is completed in seconds, while the full 3D reconstruction is accomplished in ~12 minutes using 2 GPUs. Image quality is excellent with resolution measured as FWHM of LSF of 0.8 mm for RT and 1.5 mm for IST, sound speed detectability is 7.5 m/sec and is highly linear from 1325-1700 m/sec. Sound speed is a function of tissue stiffness, analogous to but not equal to elastography. Attenuation tomograms are a function of tissue structure and composition while provide image contrast over a wide range (0-4 dB/cm/MHz) to assist in classification of masses.

B. *Clinical Evaluation*

Although more than 450 patients have been scanned with versions of IST, under the current IST/RT protocol 125 patients with an age range of 19-78 years were scanned to date. The distribution of lesions imaged is as follows: 29 simple cysts, 28 complicated cysts, 39 various solid benign, 17 cancers, 12 no findings. Mass sizes ranged from 2-39 mm. There was excellent size agreement between sonography and IST and for 13 patients who also had contrast enhanced MRI there was nearly perfect agreement of size, shape and margins to sound speed images.

The general quantitative IST attributes of masses can be summarized as follows:

- Simple cysts: low sound speed compared to water, low attenuation
- Complicated cysts: low to intermediate sound speed compared to water, low attenuation
- Solid benign masses: higher sound speed and attenuation
- Malignancies: highest sound speed and attenuation

The highest sound speed values that were measured in any patient were all associated with malignant masses, never with normal structures or benign masses. In addition, the three sets of IST/RT images provide reproducible information about mass shape, margins, volume, architectural distortion, texture, relative echogenicity, etc.

C. *Research Subject: Invasive Ductal Carcinoma*

This case was of a 33 year old woman with no family history of cancer seen for a lump or thickening of the breast. Mammography (Fig. 4, left) showed a heterogeneously dense, spiculated 2 cm mass with malignant-appearing microcalcifications in the left breast in the middle outer quadrant. Sonography (Fig. 4, right) shows at the 1:00 position in the breast, 2 cm from the nipple an irregular, heterogeneous, highly suspicious mass with an abrupt interface, 1.9x1.2 cm in diameter. Biopsy confirmed it was invasive ductal carcinoma.

Figure 4. Mammogram (left), sonogram (right)

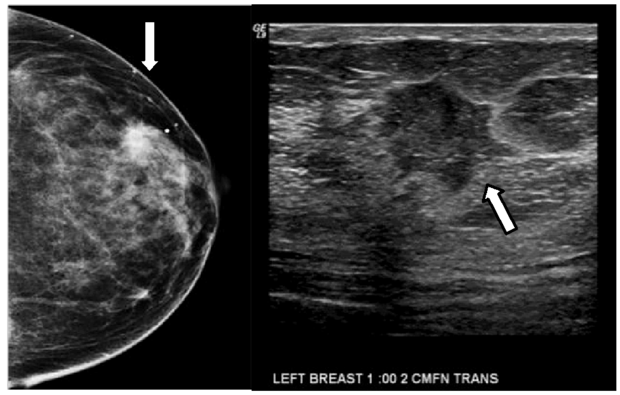

The sound speed and RT images (Fig. 5) show the mass at 1:00 in the coronal view, 2.2x1.1x1.6 cm. The mass has very high sound speed (mean 1570 m/sec), bright compared to water, high attenuation and appears hypoechoic with spiculated margins and irregular shape on the RT with architectural distortion similar to the mammogram. Precisely as the IST/RT images, the coronal T1-weighted contrast-enhanced MRI (Fig. 6) showed a mass in the same location with dimensions 2.1x1.7x1.8 cm. The fluid-filled void from the core biopsy is visible in both sound speed and MR images.

Figure 5. Sound speed IST in upper row, RT lower row. Coronal (left), cranio-caudal (middle), sagittal (right).

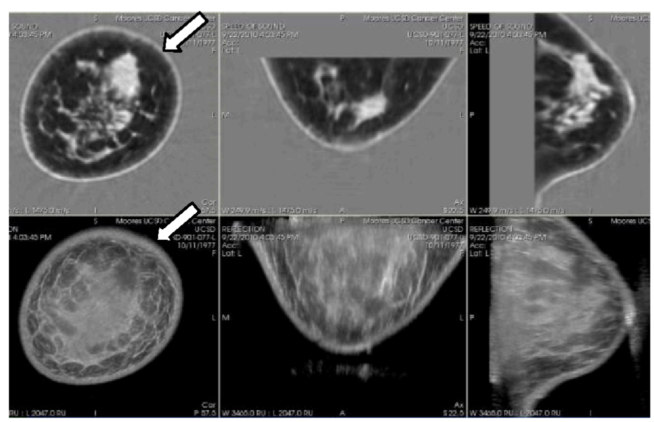

Figure 6. RT (left), sound speed (middle), T1 weighted MRI (right)

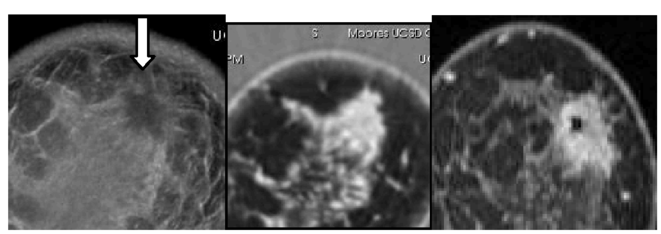

Space limitations prohibit presenting a comprehensive review of clinical findings.

V. Conclusion

The attributes of whole breast IST and RT present the following potential clinical advantages: (1) operator independence with automated scanning, (2) true anatomic breast positioning, i.e., no breast compression or distortion, (3) no ionizing radiation, (4) true quantitative 3D imaging algorithms (not just stacked 2-D images), (5) accurately registered 3D IST and RT images, (7) global views of both breasts for detailed contralateral and serial comparisons, and (8) ability to provide quantitative tissue characteristics that have thus far, not been available. These characteristics provide unique advantages in the clinical setting for applications including, but not limited to, repeat breast imaging that is safe and cost-effective, whole-breast screening for high-risk women, young women or women with dense breasts, accurate volumetric analysis for detailed surgical planning, and monitoring over time of response to surgery and therapy.

Acknowledgment

We gratefully acknowledge the support and contributions of Melissa Ledgerwood, B.S., Melanie Aiken, B.A., Laura Brogoch, B.S., Karleen Callahan, Ph.D. and the National Institutes of Health, National Cancer Institute SBIR Program.

References

[1] L. Brogoch, M. André, M. Ledgerwood, H. Ojeda-Fournier, et al., "Reader variability and predictive value of breast imaging reporting and data system descriptors for lesions in breast sonography," *J Ultrasound Med,* vol. 29, pp. S47, 2010.

[2] A. Stavros, D. Thickman, C. Rapp, et al., "Solid breast nodules: use of sonography to distinguish between benign and malignant lesions," *Radiology*, vol. 196, no. 1, pp. 123-34, 1995.

[3] A. Hong, E. Rosen, M. Soo, et al., "BI-RADS for sonography: Positive and negative predictive values of sonographic features." *AJR*, vol. 184, no. 4, pp. 1260-1265, 2005.

[4] J. Baker, P. Kornguth, M. Soo, et al., "Sonography of solid breast lesions: Observer variability of lesion description and assessment," *AJR*, vol. 172, pp. 1621-1625, 1999.

[5] W. Berg, J. Blume, J. Cormack, et al., "Operator dependence of physician performed whole breast US: Lesion detection and characterization," Radiology, vol. 241, pp. 355-365, 2006.

[6] M. Silverstein, M. Lagios, A. Recht, et al., "Image-detected breast cancer: State of the art diagnosis and treatment." *J Amer Coll Surg*, vol. 201, no. 4, pp. 586-597, 2005.

[7] M. Shetty, Y. Shah, R. Sharman, "Prospective evaluation of combined mammographic and sonographic assessment in patients with palpable abnormalities of the breast," J Ultrasound Med, vol. 22, no. 3, pp. 263-268, 2003.

[8] Y. Kwak, E. Kim, H. Park, et al., "Application of the breast imaging reporting and data system final assessment system in sonography of palpable breast lesions and reconsideration of the modified triple test," *J Ultrasound Med*, vol. 25, no. 10, pp. 1255-1261, 2006.

[9] A. T. Stavros, *Breast Ultrasound.* New York: Lippincott Williams & Wilkins, 2004, 1-1015.

[10] T. Kolb, J. Lichy and J. Newhouse, "Comparison of the performance of screening mammography, physical examination, and breast US and evaluation of factors that influence them: An analysis of 27,825 patient evaluations." *Radiology*, vol. 225, pp. 165-175, 2002.

[11] J. Greenleaf, S. Johnson, W. Samayoa and F. Duck, "Algebraic reconstruction of spatial distributions of acoustic velocities in tissue from their time-of-flight profiles," *Acoustic Holography*, vol. 6, 1975.

[12] P. Carson, C. Meyer, A. Scherzinger and T. Oughton, "Breast imaging in coronal planes with simultaneous pulse-echo and transmission ultrasound," *Science*, vol. 214, pp. 1141-1143, 1981.

[13] G. Glover, J. Sharp, "Reconstruction of ultrasound propagation speed distributions in soft tissue: Time of flight tomography," *IEEE Trans Sonics Ultrason*, vol. SU-24, pp. 229-234, 1977.

[14] J. Greenleaf, R. Bahn, "Clinical imaging with transmissive ultrasonic computerized tomography," *IEEE Trans Biomed Eng*, vol. BME-28, no. 2, pp 231, 1981.

[15] N. Duric, P. Littrup, L. Poulo, A. Babkin, et al., "Detection of breast cancer with ultrasound tomography: First results with the computed ultrasound risk evaluation prototype," *Med Phys*, vol. 34, no.2, pp. 773-785, 2007.

[16] A. Devaney, "A filtered backpropagation algorithm for diffraction tomography," *Ultrasonic Imaging*, vol. 4, pp. 336-350, 1982.

[17] M. André, H. Janee, G. Otto and P. Martin, "High speed data acquisition in a diffraction tomography system with large-scale toroidal arrays*." Int J Imaging System Technol*, vol. 8, no. 1, pp. 137-147, 1997.

[18] M. André, H. Janee, G. Otto, et al., "Reduction of phase aberration in a diffraction tomography system for breast imaging." *Acoustical Imaging*, vol. 22, pp. 151-157, 1996.

[19] Borup, D.T., S.A. Johnson, W.W. Kim, and M.J. Berggren, "Nonperturbative diffraction tomography via Gauss-Newton iteration applied to the scattering integral equation." *Ultrason Imaging*, vol. 14, no. 1, pp. 69-85, 1992.

[20] J. Wiskin, D. Borup, S. Johnson, et al., "Full wave, non-linear, inverse scattering: High resolution quantitative breast tissue tomography." *Acoustical Imaging*, vol. 28, pp. 183-194, 2007.

[21] M. André, C. Barker, N. Sekhon, J. Wiskin, D. Borup and K. Callahan, "Pre-clinical experience with full-wave inverse scattering for breast imaging: Sound speed sensitivity," *Acoustical Imaging,* vol. 29, pp. 73-80, 2008.

[22] S. Johnson, T. Abbott, R. Bell, M. Berggren, D. Borup, et al., "Non-invasive breast tissue characterization using ultrasound speed and attenuation: in vivo validation," *Acoustical Imaging*, vol. 28, pp.147-154, 2007.

[23] J. Wiskin, D. Borup, M. André, et al., "Inverse scattering results," *Acoustical Imaging*, vol. 30, pp. 61-68, 2011.

[24] J. Wiskin, D. Borup, S. Johnson, "Inverse scattering theory," *Acoustical Imaging*, vol. 30, pp. 53-60, 2011.

[25] J. Wiskin, D. Borup, S. Johnson, M. Berggren, "Nonlinear inverse scattering: High resolution quantitative breast tissue tomography" J Acoust Soc Am 131(5), pp. 3802-3813, 2012.